Organic Geochemistry 133 (2019) 10–19

Contents lists available at ScienceDirect

Organic Geochemistry

journal homepage: www.elsevier.com/locate/orggeochem

Comparison of organic and palynological proxies for biomass burning and vegetation in a lacustrine sediment record (Lake Allom, Fraser Island, Australia)

Laura T. Schreuder [a,*], Timme H. Donders [b], Anchelique Mets [a], Ellen C. Hopmans [a], Jaap S. Sinninghe Damsté [a,c], Stefan Schouten [a,c,*]

[a] NIOZ Royal Netherlands Institute for Sea Research, Department of Marine Microbiology and Biogeochemistry, and Utrecht University, P.O. Box 59, 1790 AB Den Burg, Texel, the Netherlands
[b] Palaeoecology, Laboratory of Palaeobotany and Palynology, Department of Physical Geography, Faculty of Geosciences, Utrecht University, Heidelberglaan 2, 3584CS Utrecht, the Netherlands
[c] Department of Earth Sciences, Faculty of Geosciences, Utrecht University, P.O. Box 80.121, 3508 TA Utrecht, the Netherlands

ARTICLE INFO

Article history:
Received 12 November 2018
Received in revised form 14 February 2019
Accepted 18 March 2019
Available online 19 March 2019

Keywords:
Biomass burning
Anhydrosugars
Levoglucosan
Vegetation history
Long chain *n*-alkanes
Late Holocene
Fraser Island
Southeast Queensland
Australia

ABSTRACT

Continental fire and vegetation history have been studied in sedimentary archives using palynological proxies (i.e. charcoal abundance and the pollen assemblage) and organic proxies (i.e. the anhydrosugars levoglucosan and it isomers, and plant-wax *n*-alkanes), but rarely in concert. Here, we compared palynological and organic proxies to reconstruct fire and vegetation history in a sediment core from Lake Allom on Fraser Island, Australia, covering the last 5.4 kyrs. We found that anhydrosugar and microscopic charcoal accumulation rates had similar trends, while trends in macroscopic charcoal accumulation rates were different. This was attributed to the short distance over which macroscopic charcoal is transported compared to microscopic charcoal and anhydrosugars. Furthermore, differences in fire regime and combusted types of vegetation may also explain the differences in levoglucosan and charcoal accumulation rates in lacustrine sediments. Moreover, we found that the ratios between anhydrosugars seem to be governed by combustion conditions, or by type of burned vegetation. Long chain *n*-alkane accumulation rates and stable isotope compositions showed similar patterns to the pollen assemblage throughout the last 5.4 kyrs, with both representing the local vegetation history. Collectively, our results showed that in the period between 5.4 and 4 ka, biomass burning was low on Fraser Island, while at 4 ka, fire occurrence started to increase, slightly earlier than changes in vegetation and hydrology. Therefore, we suggest that increased fire activity on Fraser Island around 4 ka might have been caused by human-lit biomass burning, since aboriginals settled on Fraser Island around this time.

1. Introduction

In the past decades, sedimentary archives have been widely studied to reconstruct continental fire history, using a variety of fire proxies (e.g. Hawthorne et al., 2017 and references therein). One of these fire proxies is based on charcoal, which is a carbonaceous material produced by heating biomass during incomplete combustion (Whitlock and Larsen, 2002). It is usually divided into two size classes: macroscopic charcoal (particles $\geq$100 μm) and microscopic charcoal (particles $\leq$100 μm). The smaller particles are assumed to be transported over longer distances compared to the larger particles and therefore macroscopic charcoal provides information on local-scale fires, while microscopic charcoal provides information on more regional-scale fires (Marlon et al., 2016; Vachula et al., 2018). The charcoal proxy has been widely used as a biomass burning indicator in lacustrine and marine sediments (e.g. Mooney and Tinner, 2011). However, application of the proxy in sedimentary archives can sometimes be challenging. For example, there are many factors determining the quantities of charcoal accumulating in lake sediments, such as lake and watershed size, the proportion of woody taxa and the burning temperatures (Kuo et al., 2008; Hawthorne et al., 2017 and references therein). Furthermore, macroscopic charcoal only provides information on local-scale fires. Another, relatively novel proxy

* Corresponding authors at: NIOZ Royal Netherlands Institute for Sea Research, Department of Marine Microbiology and Biogeochemistry, and Utrecht University, P.O. Box 59, 1790 AB Den Burg, Texel, the Netherlands (S. Schouten).
E-mail addresses: laura.schreuder@nioz.nl (L.T. Schreuder), S.Schouten1@uu.nl (S. Schouten).

https://doi.org/10.1016/j.orggeochem.2019.03.002
0146-6380/

for biomass burning is the abundance and distribution of the anhydrosugars levoglucosan (1,6-anhydro-β-D-glucose) and its isomers mannosan (1,6-anhydro-β-D-mannopyranose) and galactosan (1,6-anhydro-β-D-galactopyranose). These are thermal products of cellulose/hemicellulose generated only during vegetation burning at a temperature range of 150–350 °C (Shafizadeh et al., 1979; Simoneit et al., 1999; Kuo et al., 2011a). Levoglucosan is the most abundant anhydrosugar emitted during biomass burning and transported through the atmosphere, although its atmospheric degradation is currently under debate (e.g. Hennigan et al., 2010; Hoffmann et al., 2010; Shiraiwa et al., 2012; Lai et al., 2014; Zhao et al., 2014; Arangio et al., 2015; Pratap et al., 2018). However, levoglucosan is still considered an ideal tracer for biomass burning in aerosols because of its high emission and source-specificity (e.g. Simoneit and Elias, 2000; Bhattarai et al., 2019) and has been used in numerous air-quality studies (e.g. Iinuma et al., 2016). Levoglucosan can be transported to sedimentary archives through the atmosphere and by rivers (Hunsinger et al., 2008; Myers-Pigg et al., 2017) and is not substantially degraded during settling in the marine water column, while it is partially degraded at the marine sediment-water interface (Schreuder et al., 2018). Furthermore, ratios between levoglucosan and mannosan, and between levoglucosan, and mannosan and galactosan have been proposed to depend on the type of biomass burned (Fabbri et al., 2009) and/or on burning conditions (temperature and duration; Kuo et al., 2011a). The use of anhydrosugar proxies as biomass-burning indicators in sedimentary archives is limited (Elias et al., 2001; Kuo et al., 2011b; Lopes dos Santos et al., 2013; Sikes et al., 2013; Schüpbach et al., 2015; Shanahan et al., 2016; Battistel et al., 2017; Callegaro et al., 2018) compared to the charcoal proxies.

Palynological proxies to reconstruct past vegetation changes from lacustrine sediments are based on the assemblage of pollen grains preserved in the sediment (Sugita, 1994; Matthias and Giesecke, 2014). The pollen composition in lacustrine sediments is a distance-weighted integral of the vegetation cover surrounding the lake. However, understanding the source area of pollen and converting pollen results to estimates of plant cover can be complex and depends on pollen productivity and dispersal (Prentice, 1985). Basin size also has a strong influence on the proportion of pollen coming from local or regional sources. Generally, pollen data from smaller lakes are especially appropriate for reconstruction of local vegetation, while pollen data from larger lakes are more suitable for reconstruction of regional vegetation and climate (Sugita, 1994). Pollen analysis has been applied widely in sedimentary archives to reconstruct the vegetation history of the area around lakes (e.g. Donders et al., 2006; Kershaw et al., 2007; Donders et al., 2008). Other widely-used proxies for vegetation changes are long chain *n*-alkanes (C_{25} to C_{35}), which are compounds derived from the epicuticular wax of vascular plants (Eglinton and Hamilton, 1967). They are relatively resistant to degradation (Cranwell, 1981), making them useful as higher plant biomarkers in sediments. Plant wax alkanes typically have a strong odd/even predominance (Eglinton and Hamilton, 1963), which is expressed as the carbon preference index (CPI; Kolattukudy, 1976) and long chain *n*-alkanes from terrestrial higher plants generally have CPI values > 5 (Eglinton and Hamilton, 1963; Diefendorf et al., 2011). The chain length distribution of the alkanes, expressed as the average chain length (ACL), depends on environmental conditions and vegetation type (grasses vs. woody plants), although chain length distributions are variable within plant groups (Bush and McInerney, 2013; Diefendorf et al., 2015; Diefendorf and Freimuth, 2017 and references therein). Therefore, interpretation of the ACL of long chain *n*-alkanes can be complicated. Also, the stable carbon isotope composition of the alkanes can provide information on the abundance of C_3 and C_4 vegetation as well as on abundance of gymnosperms and angiosperms (Diefendorf and Freimuth, 2017 and references therein). Plants utilizing the C_3 photosynthetic pathway have an *n*-alkane carbon isotope composition around −36‰ (−31‰ to −39‰), while plants utilizing the C_4 photosynthetic pathway have an *n*-alkane carbon isotope composition around −21.5‰ (−18‰ to −25‰; e.g. Collister et al., 1994 and references therein; Schefuß et al., 2003; Castañeda et al., 2009; Diefendorf and Freimuth, 2017). Furthermore, the $\delta^{13}C$ of *n*-alkanes from gymnosperm trees are usually around 4‰ more enriched compared to angiosperms (Chikaraishi and Naraoka, 2003; Diefendorf et al., 2011).

Here, we present a biomass burning and vegetation record of Fraser Island, Australia, based on levoglucosan and its isomers and on long chain *n*-alkanes in Lake Allom sediments (Fig. 1). These sediments have previously been studied for vegetation and fire history over the last 54 kyrs (Donders et al., 2006) using palynological approaches, which revealed strong changes between rainforest and open woodland vegetation and increased fire occurrence during periods of drier vegetation and/or low lake levels (Donders et al., 2006). In this study, we focus on comparison of organic proxies (i.e. levoglucosan and it isomers and long chain *n*-alkanes) with palynological proxies (i.e. microscopic and macroscopic charcoal and the pollen assemblage) for vegetation and biomass burning in Lake Allom sediments during the last 5.4 kyrs. Our results shed light on the differences between these types of proxies to reconstruct vegetation and fire history in lacustrine environments, as well as on vegetation and fire history on Fraser Island over the last 5.4 kyrs.

2. Materials and methods

2.1. Site description

Fraser Island is a sand-dune island with a length of 124 km and a maximum width of 24 km, situated between 24°40′S and 25°50′S and 152°55′E and 153°20′E (Fig. 1). Annual rainfall varies between 1300 and 1700 mm/yr, and a moisture deficit occurs in the drier winter/spring season (Walker et al., 1981). Southeastern Queensland has a warm subtropical, slightly seasonal, humid climate (Webb and Tracey, 1994). Rainfall between seasons varies by about 40% and mean temperatures range from 14 °C in winter to 29 °C in summer. On Fraser Island, the perched basin named Lake Allom (25°14′S, 153°10′E) is located at the boundary between Pleistocene and Holocene parabolic dune systems, within the central rainforest belt on the island (Fig. 1c). The perched lake is approximately 300 m in length and 80 m in diameter and has a ~50-m wide fringe of littoral vegetation and has no natural in- or outflows. Surrounding vegetation units are rainforests and shrubs, wet eucalypt open forest and eucalypt woodlands to open forests (Fig. 1c). The vegetation on the island ranges from coastal shrubs and heaths on leached soils to inland layered rainforest and mixed sclerophyll vegetation on younger nutrient-rich soils. The vegetation is laterally zoned and follows the contours of successive parabolic dune systems parallel to the coastline. Fire occurs naturally on the island, especially in the *Eucalyptus*-dominated sclerophyll belt around the rainforest. More details are presented by Donders et al. (2006).

2.2. Biomarker analysis

2.2.1. Sample preparation

Lake Allom was cored and sampled in July 2003, as described previously (Donders et al., 2006). Three partly overlapping core sections were retrieved, down to 3.2 m sediment depth. The core was sampled at 1–2 cm intervals between 0 and 60 cm and at 4 cm intervals between 60 and 320 cm. The age model was based

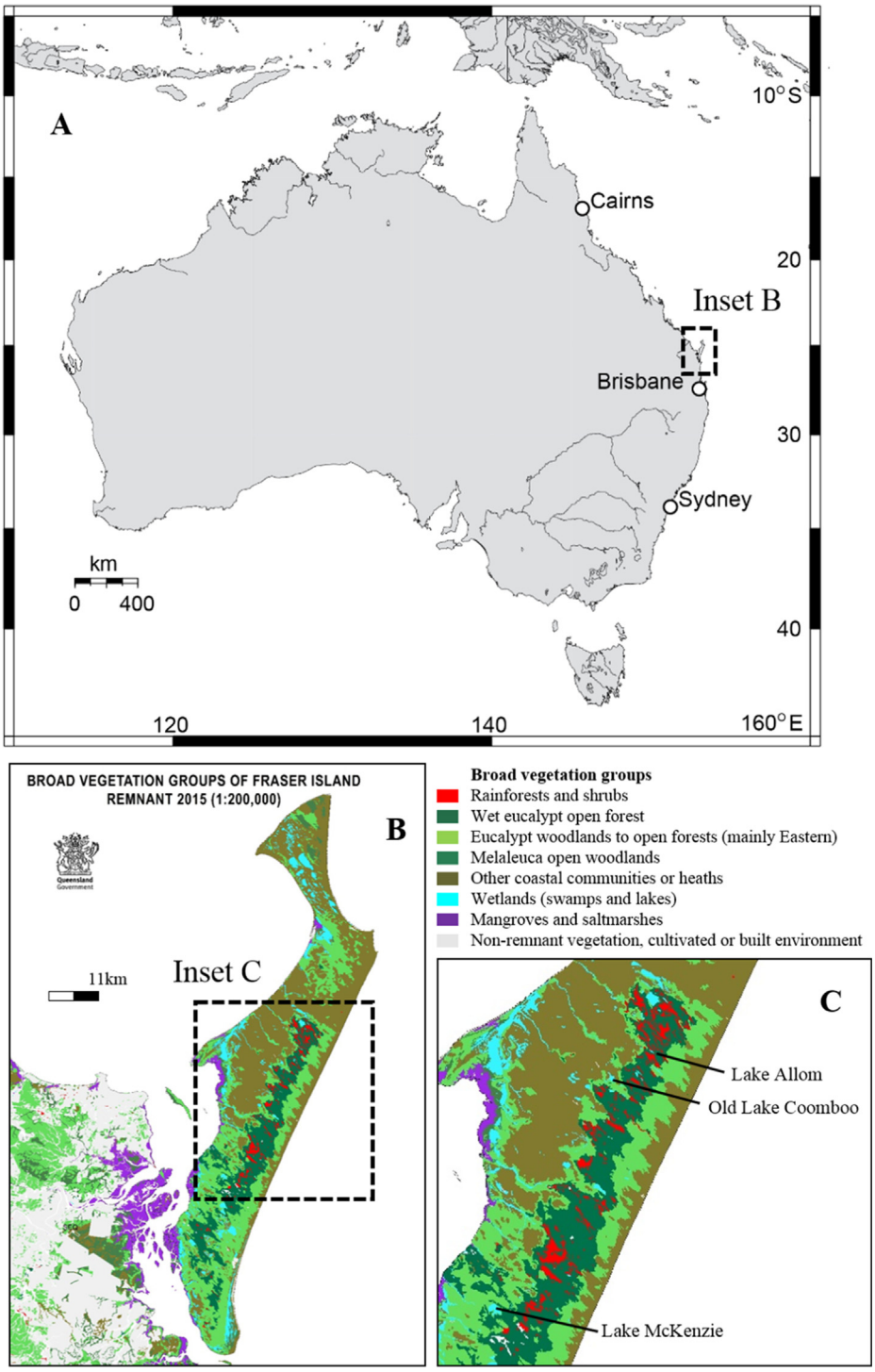

Fig. 1. (a) Location of Fraser Island off the eastern coast of Australia, (b) a zoom-in of Fraser Island on a map showing the broad vegetation groups of the island (Queensland Herbarium, 2013), and (c) a zoom-in of the island showing Lake Allom, as well as Old Lake Coomboo and Lake McKenzie.

on 16 accelerator mass spectrometry (AMS) radiocarbon dates and the record covers the last 54 kyrs, with two hiatuses at 5.8–6.8 ka and 12–33 ka (Donders et al., 2006). From these samples, 46 subsamples spanning the last 5.4 ka of the core were taken and freeze-dried and homogenized. The sediment was extracted ultrasonically (5x) with dichloromethane (DCM):methanol (MeOH) (2:1, v:v) and subsequently passed over a small Na_2SO_4 Pasteur pipette column with DCM. Each extract was split into two aliquots; one for analysis of levoglucosan and its isomers and one for long chain *n*-alkane analysis.

2.2.2. Analysis of levoglucosan and its isomers

Deuterated (D7) levoglucosan ($C_6H_3D_7O_5$; dLVG, from Cambridge Isotope Laboratories, Inc.) was added (0.5 ng) to the extracts as an internal standard to quantify levoglucosan and its isomers, after which they were dried under N_2. These aliquots were redissolved in acetonitrile: H_2O (95:5, v:v) and filtered using a regenerated cellulose filter (0.45 μm) before analysis.

Levoglucosan and its isomers were analyzed by means of ultrahigh performance liquid chromatography (UHPLC)-negative ion electrospray ionization/high resolution mass spectrometry

(ESI/HRMS) using an Agilent 1290 Infinity UHPLC coupled to an Agilent 6230 Time-Of-Flight (TOF) mass spectrometer, as described previously (Schreuder et al., 2018). Separation was achieved with two Aquity UPLC BEH amide columns (2.1 × 150 mm; 1.7 μm, Waters Chromatography) in series with a 50 mm guard column, which were kept at 30 °C. Compounds were eluted (0.2 mL/min) with 100% A (15 min), followed by back flushing with 100% B (15 min) and re-equilibration at starting conditions (25 min). Eluent A was a mixture of acetonitrile:H_2O (92.5:7.5, v:v) with 0.01% triethylamine (TEA) and eluent B was a mixture of acetonitrile:H_2O (70:30, v:v) with 0.01% TEA. Source settings for negative ion electrospray ionization (ESI) were: nebulizer P 60 psi (N_2), VCap 5 kV and drying gas (N_2) 5 L/min at a temperature of 275 °C. The monitored mass range was *m/z* 150–350. Injection volume was usually 10 μL. Levoglucosan, its isomers, and dLVG were detected as their deprotonated molecules $(M\text{-}H)^-$. Quantification was based on peak integrations of mass chromatograms within 3 ppm mass accuracy using a calculated exact mass of *m/z* 161.0445 for levoglucosan ($C_6H_{10}O_5$) and its isomers and *m/z* 168.0884 ($C_6H_3D_7O_5$) for dLVG. Authentic standards for levoglucosan, galactosan and mannosan were all obtained from Sigma Aldrich. Analytical performance and relative response factors (RRF) for levoglucosan, galactosan and mannosan compared to dLVG were determined daily by analysis of a standard mixture of levoglucosan, galactosan, mannosan and dLVG and varied between 1.20 and 1.28 for levoglucosan, between 0.63 and 0.82 for galactosan and between 0.93 and 1.09 for mannosan. The detection limit for levoglucosan was 5 pg on column. Approximately 20% of the samples were analyzed in duplicate, which resulted in an average instrumental error of 4%. Levoglucosan accumulation rates were calculated from levoglucosan concentrations using sediment accumulation rates and dry bulk densities. Dry bulk densities in the studied sediment core were assumed to be 1.0 g/cm^3.

2.2.3. Long-chain n-alkane analysis

Squalane was added to the extracts as an internal standard in order to quantify the *n*-alkanes. The extracts were separated into an apolar, a ketone and a polar fraction, on an activated Al_2O_3 column using hexane:DCM (9:1, v:v), hexane:DCM (1:1, v:v) and DCM:MeOH (1:1, v:v), respectively. The apolar fraction was further separated into an 'aliphatic' fraction, containing the *n*-alkanes, and a medium 'apolar' fraction, by passing it over an Ag^+ impregnated silica column with hexane and ethyl acetate, respectively. For *n*-alkane analysis, the 'aliphatic' fractions were dissolved in hexane and injected on-column into an Agilent 7890B gas chromatography (GC) instrument at 70 °C using an FID detector. The oven temperature was programmed to 130 °C at 20 °C/min, and subsequently to 320 °C (held 10 min) at 4 °C/min; He was the carrier gas at a constant 2 mL/min. Injection volume was 1 μL. The detection limit for *n*-alkanes was ca. 100 pg on column. Similar to levoglucosan, *n*-alkane accumulation rates were calculated from *n*-alkane concentrations.

The average chain length (ACL) and carbon preference index (CPI) of the long chain *n*-alkanes were calculated using the following formula:

$$\mathrm{ACL} = \frac{\Sigma(\mathrm{i} \times \mathrm{X_i})}{\Sigma \mathrm{X_i}}, \quad (1)$$

where X is abundance and i represents the carbon number of the *n*-alkane and ranges from 25 to 33,

$$\mathrm{CPI}_{n-\mathrm{alkanes}} = 1/2 \times \frac{\Sigma(X_{25}+X_{27}+X_{29}+X_{31}+X_{33})}{\Sigma(X_{24}+X_{26}+X_{28}+X_{30}+X_{32})} + 1/2 \times \frac{\Sigma(X_{25}+X_{27}+X_{29}+X_{31}+X_{33})}{\Sigma(X_{26}+X_{28}+X_{30}+X_{32}+X_{34})}, \quad (2)$$

according to (Kolattukudy, 1976). A high value thus indicates a high odd/even predominance.

For 4 out of 46 of the samples, the CPI could not be calculated as the even carbon numbered *n*-alkanes were below detection limit.

2.2.4. Compound specific stable carbon isotope analysis

Long chain *n*-alkanes (C_{25} to C_{33}) were analyzed for their stable carbon isotopic composition using GC–isotope ratio MS (GC–IRMS). The *n*-alkanes were analyzed using a Thermo Delta V isotope IRM mass spectrometer coupled to an Agilent 6890 GC instrument. GC conditions were as described above. The samples were analyzed in duplicate and the reported data represent the mean stable carbon isotope value of duplicate runs. The values are reported in δ notation relative to the Vienna PeeDee Belemnite (VPDB) using CO_2 reference gas calibrated to NBS-22 reference material. The instrument error was <0.5‰ based on repeated injection of external deuterated *n*-alkane standards (C_{20} and C_{24} perdeuterated *n*-alkanes) prior to and after sample analysis.

3. Results

3.1. Levoglucosan and its isomers

Levoglucosan was detected in Lake Allom sediments throughout the last 5.4 ka. Galactosan and mannosan were detected above the limit of quantitation in 36 and 37 out of 46 samples, respectively. Levoglucosan accumulation rates varied between 0.1 and 7.2 ng/cm^2/yr; galactosan accumulation rates varied between 0.03 and 1.4 ng/cm^2/yr and mannosan accumulation rates varied between 0.03 and 2.2 ng/cm^2/yr (Fig. 2a–c). The lowest accumulation of all three anhydrosugars was found in the oldest part of the record, in the period between 5.4 and 4 ka. From 4 ka to 2.2 ka, anhydrosugar accumulation rates steadily increased from ca. 0.2 to 3.5 ng/cm^2/yr for levoglucosan, from ca. 0.1 to 0.7 ng/cm^2/yr for galactosan and from ca. 0.1 to 0.6 ng/cm^2/yr for mannosan. From 2.2 ka to 0.2 ka, accumulation rates of the anhydrosugars remained relatively stable, with three peaks around 2.2, 1.4 and 1.0 ka. At ca. 0.2 ka, accumulation rates of the anhydrosugars decreased until the top of the record.

For 37 out of 46 samples, two ratios between the anhydrosugars were calculated: the ratio between levoglucosan and mannosan (L/M) varied between 2.0 and 8.0, while the ratio between levoglucosan, and galactosan and mannosan (L/G + M), varied between 0.9 and 3.5 (Fig. 2d and e). The lowest values for anhydrosugar ratios were found in the oldest part of the record, from 5.4 to approximately 4 ka, after which it steadily increased until ca. 3 ka, and remained relatively stable until the top of the record.

3.2. Long chain n-alkanes

The accumulation of long chain *n*-alkanes (C_{25}-C_{33}) varied between 0.2 and 14.6 μg/cm^2/yr (Fig. 2f) and was lowest during the period between 5.4 and 3.2 ka. From 3.2 ka to 0.9 ka, *n*-alkane accumulation steadily increased from ca. 0.2 to 14.6 μg/cm^2/yr, interrupted by a peak in accumulation at 2.7 ka. From 0.9 ka to 0.1 ka, *n*-alkane accumulation rates decreased again to ca. 6 μg/cm^2/yr. The weighted mean $\delta^{13}C$ of the long chain *n*-alkanes varied between −33.1 and −30.0‰. However, since the C_{29} *n*-alkane was most abundant and therefore gives the most reliable $\delta^{13}C$ record, we focused only on the $\delta^{13}C$ record of the C_{29} *n*-alkane. These values varied between −33.0 and −28.5‰ and were most depleted during the period between 5.4 and 3.5 ka (Fig. 2g). From 3.5 ka until 2.7 ka, $\delta^{13}C$ increased from ca. −32‰ to ca. −29.5‰ and remained relatively stable until the top of the record. The ACL values of the *n*-alkanes were on average 29.9 ± 0.2 and

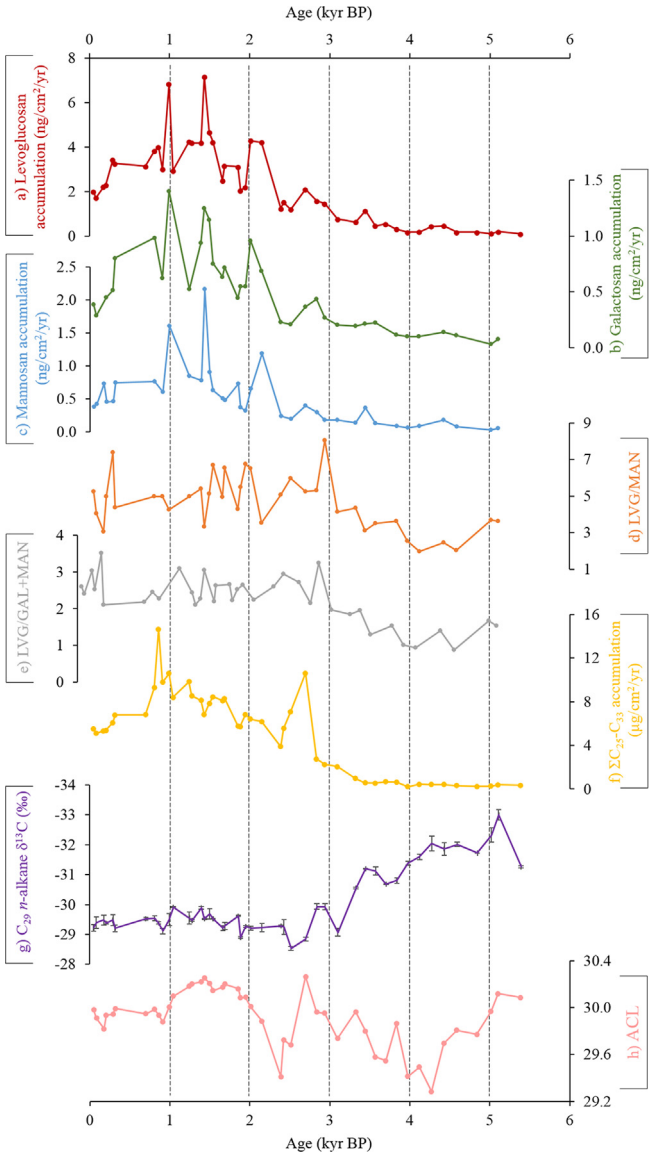

Fig. 2. Comparison of geochemical records from the Lake Allom core: (a) levoglucosan accumulation rate, (b) galactosan accumulation rate, (c) mannosan accumulation rate, (d) ratio between levoglucosan and mannosan (LVG/MAN), (e) ratio between levoglucosan, and galactosan and mannosan (LVG/GAL + MAN), (f) accumulation rate of the sum of odd-numbered long-chain *n*-alkanes (C_{25-33}), (g) $\delta^{13}C$ of the C_{29} *n*-alkane and (h) average chain length (ACL) of *n*-alkanes (C_{25-33}) (Eq. (1)). The isotope data are reported in delta notation (‰) against the VPDB standard.

fluctuated between 29.3 and 30.3 throughout the last 5.4 ka (Fig. 2h). The CPI values of the *n*-alkanes varied from 2.4 to 33.2 and were on average 12.2 ± 6.5.

4. Discussion

4.1. Comparison of palynological and organic proxies

4.1.1. Biomass burning proxies

Fire history of the last 5.4 kyrs on Fraser Island has previously been studied using microscopic charcoal (10–120 µm) and macroscopic charcoal (120–250 µm and >250 µm) in 79 samples in the same core from Lake Allom (Donders et al., 2006). Microscopic charcoal accumulations were based on counted charcoal particle concentrations, while macroscopic charcoal accumulations were based on the area of charcoal particles per sample. Here, we compared these charcoal particle classes with levoglucosan accumulation rates and anhydrosugar ratios (L/M and L/G + M) obtained from 46 of these same samples. We focused only on levoglucosan accumulation rates and not on accumulation rates of galactosan or mannosan because (a) galactosan and mannosan were only detected in 36 and 37 out of 46 samples, respectively, (b) levoglucosan, mannosan and galactosan accumulation have similar trends (Fig. 2a–c) and (c) levoglucosan is the most abundant anhydrosugar.

Levoglucosan accumulation and microscopic charcoal have similar trends over the past 5.4 ka (Fig. 3a and d), and are significantly correlated ($R^2 = 0.159$ and $p < 0.050$). This is not unexpected, since both levoglucosan and microscopic charcoal usually represent a more regional biomass burning signal, given that these compounds can be associated with fine particulate matter and can be transported over longer distances (Simoneit et al., 1999; Marlon et al., 2016 and references therein; Myers-Pigg et al., 2016; Schreuder et al., 2018). On the other hand, macroscopic charcoal accumulation in Lake Allom is very different from levoglucosan accumulation (Fig. 3a, e and f) and there is no significant correlation between accumulation of levoglucosan and macroscopic charcoal particles with a size between 120 and 250 µm ($R^2 = 0.004$, $p = 0.682$) and macroscopic charcoal particles larger than 250 µm ($R^2 = 0.000$, $p = 0.911$). This may be explained by the much shorter distance over which macroscopic charcoal is transported, compared to levoglucosan (Marlon et al., 2016 and references therin). Therefore, accumulation of macroscopic charcoal particles represents a local fire signal, while accumulation of levoglucosan and microscopic charcoal represent a more regional fire signal. However, it is yet unclear what the size (i.e. distance from lake) of the 'regional' source area for levoglucosan and microscopic charcoal is, and whether these particles are even derived from Fraser Island, or from the adjacent Australian continent. Although levoglucosan can be transported through the atmosphere over hundreds of kilometers (e.g. Schreuder et al., 2018), it seems most likely that the source area of levoglucosan and microscopic charcoal in Lake Allom is on Fraser Island, since the direction of the prevailing winds in this region is from the southeast (Australian Bureau of Meteorology, 2013) and the Australian continent is located ~40 km away from Lake Allom. Therefore, we hypothesize that levoglucosan and microscopic charcoal represent the fire history on Fraser Island, rather than of the Australian continent. Previous studies have also examined the relationship between levoglucosan and charcoal of different size classes. For example, in lake sediments in Brazil, levoglucosan concentrations correlated with total counted charcoal concentrations (Elias et al., 2001), while for lake sediments in Ghana, levoglucosan accumulation rates correlated with accumulation rates of charcoal particles larger than 5 µm (Shanahan et al., 2016). Argiriadis et al. (2018) found that levoglucosan fluxes correlated with total charcoal fluxes in lake sediments in New Zealand, although not all peaks in levoglucosan coincide with peaks in charcoal. In contrast, Sikes et al. (2013) did not find any relationship between charcoal particle (>5 µm) concentration and levoglucosan concentration in a maar lake in New Zealand, while Schüpbach et al. (2015) also did not find a clear relationship between levoglucosan concentration and the concentration of macroscopic charcoal. The relationship between charcoal and levoglucosan accumulation in lacustrine environments thus seems to be highly variable and probably depends on local conditions. For example, the larger the basin size, the larger the proportion of regional long-distance input, but this does not explain all of the variation between levoglucosan and charcoal accumulation in the different lakes.

Another factor that may explain the variability in the relationship between levoglucosan and charcoal is the combustion temperature of fires at the different locations and time periods.

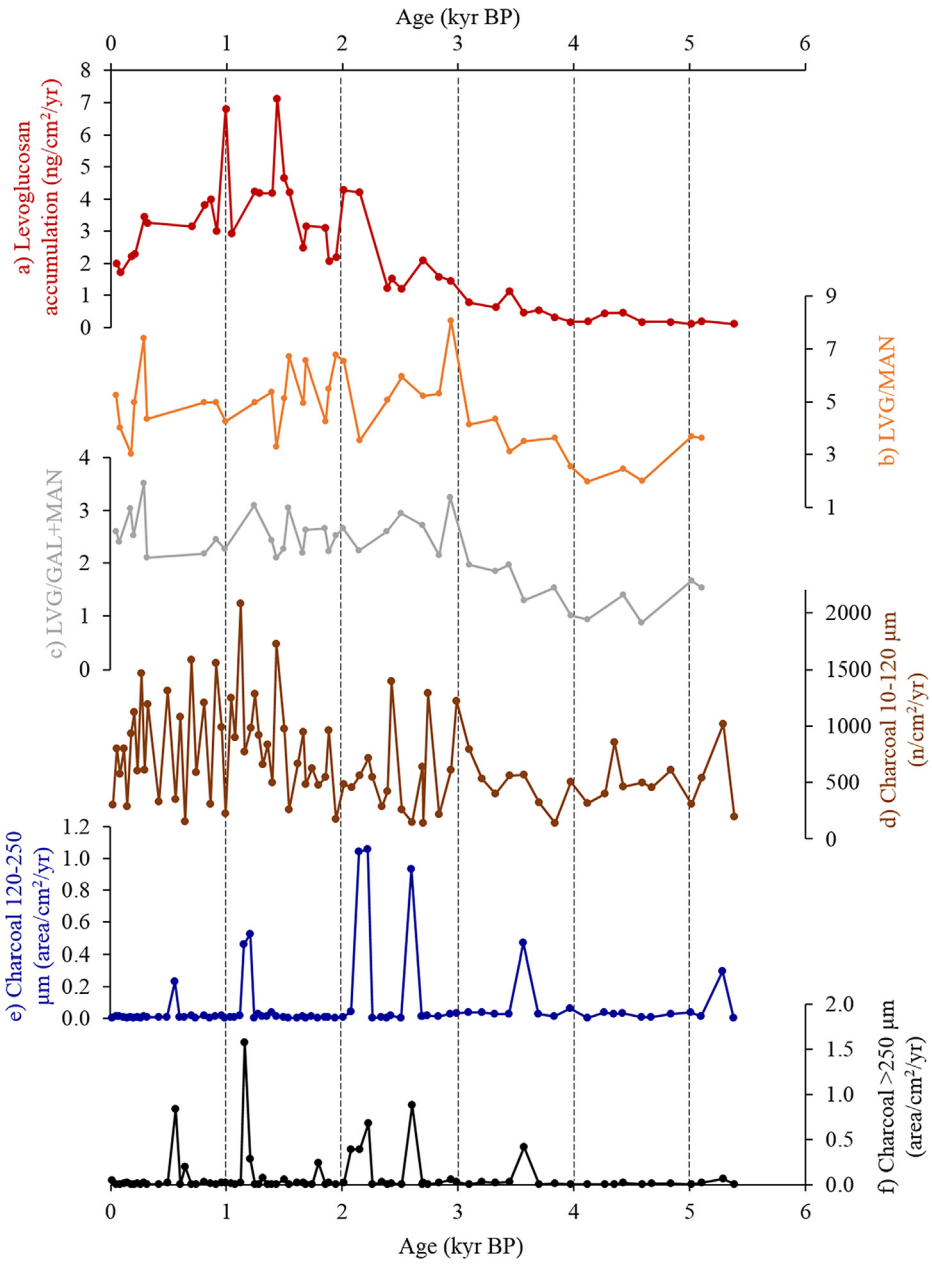

Fig. 3. Comparison of organic and palynological fire proxies: (a) levoglucosan accumulation rate, (b) ratio between levoglucosan and mannosan (LVG/MAN), (c) ratio between levoglucosan, and galactosan and mannosan (LVG/GAL + MAN), (d) microscopic charcoal (10–120 µm) accumulation rate (from Donders et al., 2006), (e) macroscopic charcoal (120–250 µm) accumulation rate (from Donders et al., 2006) and (f) macroscopic charcoal (>250 µm) accumulation rate (from Donders et al., 2006).

Levoglucosan is formed at a temperature range of 150–350 °C, while charcoal formation is more prevalent at higher temperatures (Kuo et al., 2008; Kuo et al., 2011a). Therefore, differences in fire regime could result in varying amounts of levoglucosan and charcoal produced. For example, smoldering fires are lower temperature fires compared to flaming fires and therefore it is likely that more levoglucosan is produced during smoldering fires than during flaming fires. Also, when fires occur regularly and vegetation is fire-adapted, as it is typically in Australia, fuel cannot accumulate and fires are less severe and of lower temperature. Fire frequency can therefore also influence levoglucosan and charcoal formation (Harrison et al., 2010).

Furthermore, the mode of transport of particles into the lake environment can also affect charcoal and levoglucosan accumulation. For example, large river inflow during seasonal floods could cause larger charcoal particles to be transported to lake sediments. Also, both levoglucosan and charcoal production are also influenced by the type of plant material that is combusted (Kuo et al., 2008; Kuo et al., 2011a), possibly also resulting in varying amounts of levoglucosan and charcoal produced at the different locations.

The two anhydrosugar ratio values started to increase at approximately 4 ka, concurrent with the increase in levoglucosan accumulation (Fig. 3a–c). This could either be due to differences in combustion conditions (Kuo et al., 2011a), or due to different types of vegetation burned (e.g. Fabbri et al., 2009; Alves et al., 2010). In our study, the anhydrosugar ratio values increased at approximately the same time as the increase in biomass burning and the change in vegetation (Fig. 2f and g, and Donders et al., 2006).

Therefore, both combustion conditions and the type of vegetation that was burned, could influence anhydrosugar ratios around Lake Allom.

4.1.2. Vegetation proxies

The CPI values for the *n*-alkanes are on average 12.2, indicating that the alkanes are predominantly derived from terrestrial higher plants (Eglinton and Hamilton, 1963; Diefendorf et al., 2011). We compared the pollen assemblages, previously reported by Donders et al. (2006), with the long chain *n*-alkane accumulation rates, the $\delta^{13}C$ of the C_{29} *n*-alkane and the ACL of the alkanes (Fig. 4). At ca. 3.2 ka in Lake Allom, gymnosperm tree pollen begins to increase, while angiosperm tree pollen declines comparatively (Fig. 4d). At approximately the same time, long chain *n*-alkane accumulation increased (Fig. 4a). At first glance this seems unexpected, since long chain *n*-alkane abundances are typically lower in gymnosperms (and more specifically conifers) than in angiosperms (Diefendorf and Freimuth, 2017 and references therein). However, long chain *n*-alkane abundances can vary strongly within gymnosperm vegetation (Diefendorf and Freimuth, 2017 and references therein). Indeed, gymnosperm tree pollen in Lake Allom is mainly dominated by that of the Araucariaceae (Donders et al., 2006), and this vegetation group can become very large and produces high amounts of long chain *n*-alkanes, similar to those of angiosperms (Diefendorf and Freimuth, 2017 and references therein). Therefore, the increase in *n*-alkane accumulation rates concurrent with the increase in gymnosperm tree pollen at ca. 3.2 ka can be explained by the increase in Araucariaceae vegetation. At approximately the same time, the $\delta^{13}C$ value of the C_{29} *n*-alkane shifts from ca. −32‰ to ca. −29.5‰ (Fig. 4b). Usually, plants utilizing the C_3 photosynthetic pathway have an *n*-alkane carbon isotope composition around −36‰ (−31‰ to −39‰), while plants utilizing the C_4 photosynthetic pathway have an *n*-alkane carbon isotope composition around −21.5‰ (−18‰ to −25‰; e.g. Collister et al., 1994; Schefuß et al., 2003; Castañeda et al., 2009; Diefendorf and Freimuth, 2017). However, in this case the data probably do not a C_3 vs. C_4 plant signal, since the pollen assemblage shows large variability in angiosperm and gymnosperm tree pollen, while non-arboreal pollen abundances hardly vary over the past 5.4 ka (Fig. 4d). It is therefore more likely that

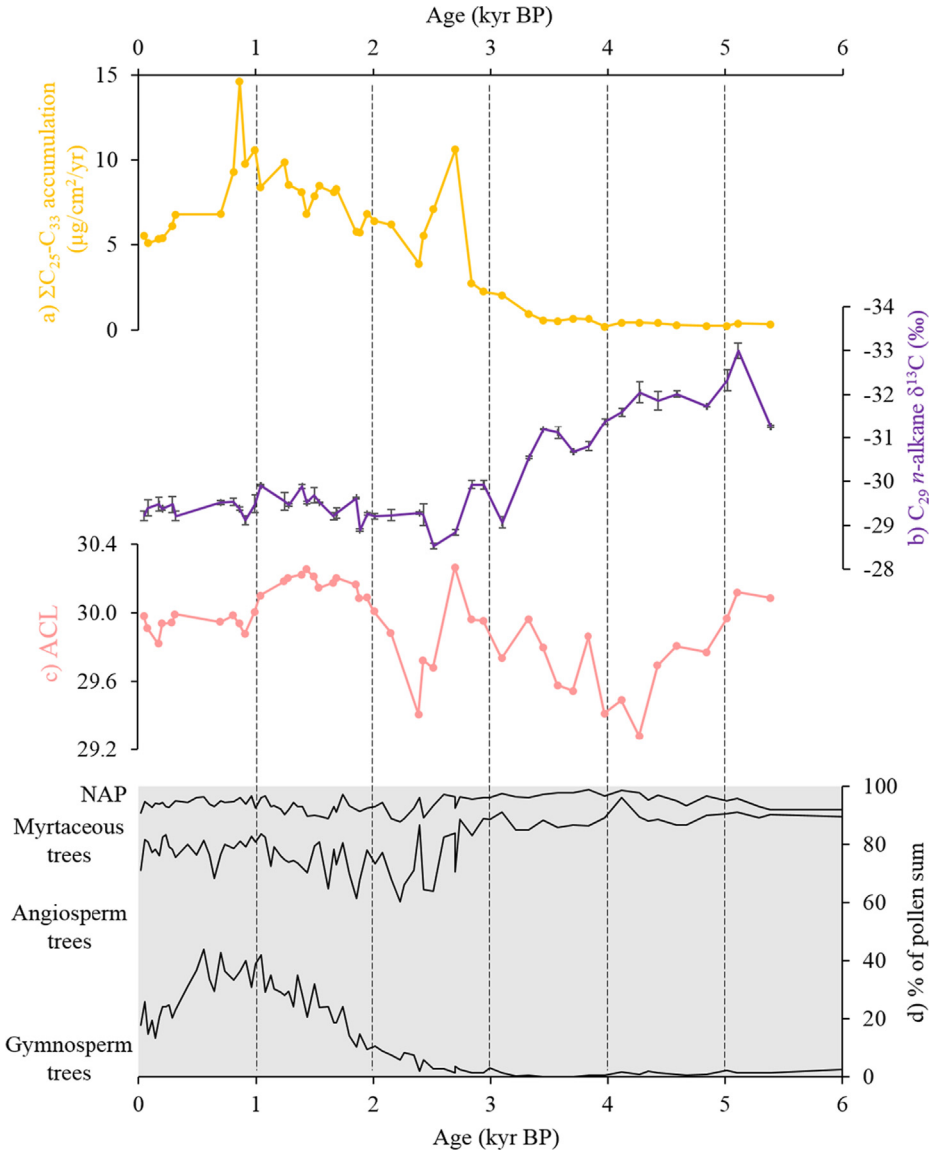

Fig. 4. Comparison of organic and palynological vegetation proxies: (a) odd-numbered long-chain *n*-alkane (C_{25-33}) accumulation rate, (b) $\delta^{13}C$ of the C_{29} *n*-alkane and (c) average chain length (ACL) of *n*-alkanes (C_{25-33}) (Eq. (1)) and (d) percentage pollen diagram (from Donders et al., 2006).

$\delta^{13}C$ of the C_{29} *n*-alkane represents an angiosperms vs. gymnosperms signal, instead of a C_3 vs. C_4 signal. Indeed, the $\delta^{13}C$ values of the C_{29} *n*-alkane increased ~2.5‰, concurrent with a ~40% increase in gymnosperm tree pollen and a ~ 40% decrease in angiosperm tree pollen (Fig. 4b and d). This is in line with earlier studies which found that the $\delta^{13}C$ values of *n*-alkanes from gymnosperm trees were usually around 4‰ more enriched, compared to those of angiosperms (Chikaraishi and Naraoka, 2003; Diefendorf et al., 2011). The ACL of the *n*-alkanes does not show a change around 3.2 ka, but fluctuates throughout the last 5.4 ka (Fig. 4c). This indicates that variations in the ACL are not reflecting changes in vegetation, which is in agreement with previous work that showed that the ACL of long chain *n*-alkanes is variable within plant species and with environmental factors (Bush and McInerney, 2013; Diefendorf et al., 2015; Diefendorf and Freimuth, 2017 and references therein). The pollen assemblage and the long chain *n*-alkanes thus show similar vegetation patterns throughout the last 5.4 kyrs. Pollen is transported to Lake Allom over relatively short distances, from ca. 600–800 m around the lake (Sugita, 1994; Donders et al., 2006), while long chain *n*-alkanes in lake sediments are thought to also be predominantly transported from vegetation in the immediate watershed (Rieley et al., 1991; Schwark et al., 2002); although long-range transport of *n*-alkanes is also possible (Gagosian and Peltzer, 1986). Taking into consideration that the current vegetation on Fraser Island is heterogeneous (Fig. 1) and that other vegetation records on Fraser Island show different vegetation history over the same time period (Longmore, 1997; Longmore and Heijnis, 1999; Atahan et al., 2015), our data suggest that the long chain *n*-alkanes are transported from a (local) source area, similar to that of the pollen source area and that both record the local vegetation history.

4.2. Reconstruction of biomass burning on Fraser Island

As discussed in the previous paragraphs, the anhydrosugar and long chain *n*-alkane records herein provide information on biomass burning and vegetation changes, respectively, on Fraser Island over the last 5.4 kyrs. In the period between 5.4 and 4 ka, anhydrosugar accumulation rates and ratios were low, indicating low fire activity in this time period (Fig. 2a–e). At ca. 4 ka, anhydrosugar accumulation rates and ratios started to increase (Fig. 2a–e), suggesting that at this time, biomass burning on Fraser Island increased. Increased biomass burning at ca. 4 ka was also recorded by charcoal in lake sediments located ca. 5 km further southwest on Fraser Island (Old Lake Coomboo; Fig. 1c) (Longmore, 1997; Longmore and Heijnis, 1999). In contrast, a lake charcoal record located on the southern part of Fraser Island (Lake McKenzie; Fig. 1c), did not reveal an increase in biomass burning around 4 ka (Atahan et al., 2015). However, the Lake McKenzie record does not contain information on short-term alterations in fire activity, as the time resolution for each sample is low (Atahan et al., 2015). Therefore, it might be possible that the biomass burning increase at ca. 4 ka as shown in the Lake Allom record is not visible in the Lake McKenzie record. Furthermore, the source area of microscopic charcoal to lake McKenzie is likely to be different, since the lake is located ca. 30 km southwest of Lake Allom. Hence, these lake sediments likely recorded changes in a slightly different area on Fraser Island than those recorded in Lake Allom sediments. Also, Lake Allom and Old Lake Coomboo are located closer to the more fire-prone heath/shrub vegetation than Lake McKenzie. The agreement between the Old Lake Coomboo charcoal record and our anhydrosugar records implies that the anhydrosugar records of the Lake Allom core represent biomass burning on (the northern part of) Fraser Island and that biomass burning increased from ca. 4 ka.

Fire occurrence on Fraser Island can be impacted by several factors, including vegetation composition and abundance. A major shift in vegetation type around Lake Allom occurred at ca. 3.2 ka, when it changed to the present-day heterogeneous sub-tropical Araucarian (gymnosperm) rainforest (Fig. 4 and Donders et al., 2006). This vegetation change was suggested to be caused by a change in the hydrological cycle, likely related to intensification of the El Niño-Southern Oscillation (ENSO) (Donders et al., 2006). The earlier Late Pleistocene and Holocene study of Lake Allom sediments indicated that this change in vegetation type occurred synchronously with an increase in fire activity (Donders et al., 2006). Our results show approximately the same, although it seems that anhydrosugar accumulation rates and ratios increased slightly earlier than the vegetation shift (Fig. 2). This suggests that biomass burning might have increased in absence of changes in vegetation type and related changes in the hydrological cycle/ENSO dynamics, which increased in approximately two steps; around 5 ka and 3 ka (Donders et al., 2007; Donders et al., 2008). Therefore, we hypothesize that there could also be another factor influencing fire occurrence on Fraser Island at that time.

This factor may be the human influence on fire occurrence, as found for a number of locations in northeast Queensland (e.g. Kershaw, 1986; Kershaw et al., 2003; Haberle, 2005), and also for the near-by North Stradbroke Island (Moss et al., 2013). Indeed, archaeological investigations indicate human occupation of the mainland adjacent to Fraser Island to date to at least ca. 5.5 ka (McNiven et al., 2002) and occupation of Fraser Island itself was dated at ca. 3 ka (McNiven et al., 2002; Ulm, 2011). Since the increase in biomass burning at ca. 4 ka is possibly not related to changes in vegetation and the hydrological cycle/ENSO dynamics, and since aboriginal people started to occupy the island around this time, we hypothesize that human occupation of the island might have caused the increase in fire activity at ca. 4 ka. When aboriginals arrived on Fraser Island, angiosperm trees (mainly *Casuarina*) dominated the vegetation around Lake Allom and, therefore, this vegetation type was the available fuel for Aboriginal fire practices. The subsequent decrease in *Casuarina* trees around 3.2 ka could have been a result of increased Aboriginal fire activity on the island, since these trees are not well adapted to fire (Hyland, 1983). At the same time, a prominent rise in Araucarian rainforest occurred around Lake Allom. At first glance, this seems remarkable, since Araucarian vegetation is also not well adapted to fire (Kershaw, 1994) and other fire studies in Queensland have suggested that Aboriginal fires were responsible for a decrease in Araucarian rainforest (Kershaw, 1986; Kershaw, 1994). However, a study of Aboriginal land and fire management suggested that rainforest conservation was valued to a high degree (Hill et al., 2000). Therefore, the Araucarian rainforest on Fraser Island might have been protected from Aboriginal fire practices and, possibly, other parts of the island outside of the rainforest belt, experienced greater fire disturbance. A fire record from Lake McKenzie, on the southern part of Fraser Island, showed no link between Late Holocene biomass burning and human occupation (Atahan et al., 2015). However, since the vegetation on Fraser Island is highly heterogeneous (Donders et al., 2006), and therefore probably fire occurrence as well, it might be that biomass burning was less abundant on the southern part of the island.

5. Conclusions

Anhydrosugars (levoglucosan and its isomers) and long chain *n*-alkanes were measured in lacustrine sediments on Fraser Island, Australia, as proxies for biomass burning and vegetation composition, and were compared to data for palynological proxies. We found that anhydrosugar accumulation and microscopic charcoal have similar trends, while macroscopic charcoal was very different. This is attributed to the short distances over which macroscopic

charcoal is transported compared to both microscopic charcoal and anhydrosugars, which are transported over longer distances and therefore represent more regional biomass burning. We also found that the ratios between the anhydrosugars could be governed by combustion conditions and by differences in vegetation types burned. Long chain *n*-alkane accumulation, the stable isotope composition of the C_{29} *n*-alkane and the pollen assemblage, show similar patterns throughout the last 5.4 kyrs. Since pollen are transported to Lake Allom over relatively short distances, and taking into consideration that the vegetation on Fraser Island is heterogeneous, the correspondence between the *n*-alkanes and the pollen implies that the plant-wax *n*-alkanes are also transported from a similar local source area, and that they record the local vegetation history.

Our results show that in the period between 5.4 and 4 ka, biomass burning was low on Fraser Island, while at 4 ka, fire occurrence started to increase. This biomass burning intensification occurred slightly earlier than the shift in vegetation around Lake Allom to the present-day heterogeneous sub-tropical Araucarian (gymnosperm) rainforest. This suggests that fire occurrence on Fraser Island might have increased in absence of changes in vegetation and related changes in the hydrological cycle and that there could be another factor influencing biomass burning on Fraser Island at this time. We suggest that increased fire activity on Fraser Island around 4 ka might have been caused by human-lit fires, since aboriginals settled on Fraser Island around this time. Furthermore, since increased biomass burning precluded the change to Araucarian rainforest vegetation, we suggest that Aboriginal-lit fires as well as rainforest conservation by aboriginals, might have influenced vegetation change on Fraser Island.

6. Declarations of interest

None.

Acknowledgements

We thank Friederike Wagner, Ton van Druten, Wolfram Kürschner and Dan Schwartz for their help collecting the sediment cores. Also, the Queensland Environmental Protection Agency, Raphael Wust from James Cook University, the CSIRO Tropical Forest Research Centre in Atherton, Qld are thanked for fieldwork support. Tim Ryan of the Queensland Herbarium is acknowledged for providing Fraser Island vegetation maps. The research was funded by The Netherlands Organization for Scientific Research (NWO; project 824.14.001). S.S. and J.S.S.D. are supported by the Netherlands Earth System Science Center (NESSC) funded by the Dutch Ministry of Science, Culture and Education.

Associate Editor—**Stuart Wakeham**

References

Australian Bureau of Meteorology, 2013. Australian Government. http://www.bom.gov.au/.

Alves, C., Gonçalves, C., Evtyugina, M., Pio, C., Mirante, F., Puxbaum, H., 2010. Particulate organic compounds emitted from experimental wildland fires in a Mediterranean ecosystem. Atmospheric Environment 44, 2750–2759.

Arangio, A.M., Slade, J.H., Berkemeier, T., Pöschl, U., Knopf, D.A., Shiraiwa, M., 2015. Multiphase chemical kinetics of OH radical uptake by molecular organic markers of biomass burning aerosols: humidity and temperature dependence, surface reaction, and bulk diffusion. The Journal of Physical Chemistry A 119, 4533–4544.

Argiriadis, E., Battistel, D., McWethy, D.B., Vecchiato, M., Kirchgeorg, T., Kehrwald, N., Whitlock, C., Wilmshurst, J.M., Barbante, C., 2018. Lake sediment fecal and biomass burning biomarkers provide direct evidence for prehistoric human-lit fires in New Zealand. Scientific Reports 8, 12113.

Atahan, P., Heijnis, H., Dodson, J., Grice, K., Le Metayer, P., Taffs, K., Hembrow, S., Woltering, M., Zawadzki, A., 2015. Pollen, biomarker and stable isotope evidence of late Quaternary environmental change at Lake McKenzie, southeast Queensland. Journal of Paleolimnology 53, 139–156.

Battistel, D., Argiriadis, E., Kehrwald, N., Spigariol, M., Russell, J.M., Barbante, C., 2017. Fire and human record at Lake Victoria, East Africa, during the Early Iron Age: Did humans or climate cause massive ecosystem changes? The Holocene 27, 997–1007.

Bhattarai, H., Saikawa, E., Wan, X., Zhu, H., Ram, K., Gao, S., Kang, S., Zhang, Q., Zhang, Y., Wu, G., 2019. Levoglucosan as a tracer of biomass burning: Recent progress and perspectives. Atmospheric Research 220, 20–33.

Bush, R.T., McInerney, F.A., 2013. Leaf wax *n*-alkane distributions in and across modern plants: implications for paleoecology and chemotaxonomy. Geochimica et Cosmochimica Acta 117, 161–179.

Callegaro, A., Battistel, D., Kehrwald, N.M., Matsubara Pereira, F., Kirchgeorg, T., Villoslada Hidalgo, M.D.C., Bird, B.W., Barbante, C., 2018. Fire, vegetation, and Holocene climate in a southeastern Tibetan lake: a multi-biomarker reconstruction from Paru Co. Climate of the Past 14, 1543–1563.

Castañeda, I.S., Mulitza, S., Schefuß, E., Lopes dos Santos, R.A., Sinninghe Damsté, J.S., Schouten, S., 2009. Wet phases in the Sahara/Sahel region and human migration patterns in North Africa. Proceedings of the National Academy of Sciences 106, 20159–20163.

Chikaraishi, Y., Naraoka, H., 2003. Compound-specific δD–$\delta^{13}C$ analyses of *n*-alkanes extracted from terrestrial and aquatic plants. Phytochemistry 63, 361–371.

Collister, J.W., Rieley, G., Stern, B., Eglinton, G., Fry, B., 1994. Compound-specific $\delta^{13}C$ analyses of leaf lipids from plants with differing carbon dioxide metabolisms. Organic Geochemistry 21, 619–627.

Cranwell, P., 1981. Diagenesis of free and bound lipids in terrestrial detritus deposited in a lacustrine sediment. Organic Geochemistry 3, 79–89.

Diefendorf, A.F., Freeman, K.H., Wing, S.L., Graham, H.V., 2011. Production of *n*-alkyl lipids in living plants and implications for the geologic past. Geochimica et Cosmochimica Acta 75, 7472–7485.

Diefendorf, A.F., Freimuth, E.J., 2017. Extracting the most from terrestrial plant-derived *n*-alkyl lipids and their carbon isotopes from the sedimentary record: A review. Organic Geochemistry 103, 1–21.

Diefendorf, A.F., Leslie, A.B., Wing, S.L., 2015. Leaf wax composition and carbon isotopes vary among major conifer groups. Geochimica et Cosmochimica Acta 170, 145–156.

Donders, T.H., Haberle, S.G., Hope, G., Wagner, F., Visscher, H., 2007. Pollen evidence for the transition of the Eastern Australian climate system from the post-glacial to the present-day ENSO mode. Quaternary Science Reviews 26, 1621–1637.

Donders, T.H., Wagner-Cremer, F., Visscher, H., 2008. Integration of proxy data and model scenarios for the mid-Holocene onset of modern ENSO variability. Quaternary Science Reviews 27, 571–579.

Donders, T.H., Wagner, F., Visscher, H., 2006. Late Pleistocene and Holocene subtropical vegetation dynamics recorded in perched lake deposits on Fraser Island, Queensland, Australia. Palaeogeography, Palaeoclimatology, Palaeoecology 241, 417–439.

Eglinton, G., Hamilton, R., 1963. The distribution of alkanes. Chemical Plant Taxonomy 187, 217.

Eglinton, G., Hamilton, R.J., 1967. Leaf epicuticular waxes. Science 156, 1322–1335.

Elias, V.O., Simoneit, B.R., Cordeiro, R.C., Turcq, B., 2001. Evaluating levoglucosan as an indicator of biomass burning in Carajas, Amazonia: A comparison to the charcoal record. Geochimica et Cosmochimica Acta 65, 267–272.

Fabbri, D., Torri, C., Simoneit, B.R., Marynowski, L., Rushdi, A.I., Fabiańska, M.J., 2009. Levoglucosan and other cellulose and lignin markers in emissions from burning of Miocene lignites. Atmospheric Environment 43, 2286–2295.

Gagosian, R.B., Peltzer, E.T., 1986. The importance of atmospheric input of terrestrial organic material to deep sea sediments. Organic Geochemistry 10, 661–669.

Haberle, S.G., 2005. A 23,000-yr pollen record from Lake Euramoo, wet tropics of NE Queensland, Australia. Quaternary Research 64, 343–356.

Harrison, S.P., Marlon, J.R., Bartlein, P.J., 2010. Fire in the Earth system. In: Dodson, John (Ed.), Changing Climates, Earth Systems and Society. Springer, Dordrecht, pp. 21–48.

Hawthorne, D., Mustaphi, C.J.C., Aleman, J.C., Blarquez, O., Colombaroli, D., Daniau, A.-L., Marlon, J.R., Power, M., Vannière, B., Han, Y., 2017. Global Modern Charcoal Dataset (GMCD): A tool for exploring proxy-fire linkages and spatial patterns of biomass burning. Quaternary International 488, 3–17.

Hennigan, C.J., Sullivan, A.P., Collett, J.L., Robinson, A.L., 2010. Levoglucosan stability in biomass burning particles exposed to hydroxyl radicals. Geophysical Research Letters 37, 1–4.

Hill, R., Griggs, P., Incorporated, B.B.N., 2000. Rainforests, agriculture and Aboriginal fire-regimes in wet tropical Queensland, Australia. Australian Geographical Studies 38, 138–157.

Hoffmann, D., Tilgner, A., Iinuma, Y., Herrmann, H., 2010. Atmospheric stability of levoglucosan: a detailed laboratory and modeling study. Environmental Science & Technology 44, 694–699.

Hunsinger, G.B., Mitra, S., Warrick, J.A., Alexander, C.R., 2008. Oceanic loading of wildfire-derived organic compounds from a small mountainous river. Journal of Geophysical Research, Biogeosciences 113, 1–14.

Hyland, B., 1983. Germination, growth and mineral ion concentrations of Casuarina species under saline conditions. Australian Journal of Botany 31, 1–9.

Iinuma, Y., Keywood, M., Herrmann, H., 2016. Characterization of primary and secondary organic aerosols in Melbourne airshed: The influence of biogenic emissions, wood smoke and bushfires. Atmospheric Environment 130, 54–63.

Kershaw, A., 1994. Pleistocene vegetation of the humid tropics of northeastern Queensland, Australia. Palaeogeography, Palaeoclimatology, Palaeoecology 109, 399–412.

Kershaw, A., van Der Kaars, S., Moss, P., 2003. Late Quaternary Milankovitch-scale climatic change and variability and its impact on monsoonal Australasia. Marine Geology 201, 81–95.
Kershaw, A.P., 1986. Climatic change and Aboriginal burning in north-east Australia during the last two glacial/interglacial cycles. Nature 322, 47–49.
Kershaw, A.P., Bretherton, S.C., van der Kaars, S., 2007. A complete pollen record of the last 230 ka from Lynch's Crater, north-eastern Australia. Palaeogeography, Palaeoclimatology, Palaeoecology 251, 23–45.
Kolattukudy, P.E., 1976. Chemistry and Biochemistry of Natural Waxes. Elsevier Scientific Pub Co.
Kuo, L.-J., Herbert, B.E., Louchouarn, P., 2008. Can levoglucosan be used to characterize and quantify char/charcoal black carbon in environmental media? Organic Geochemistry 39, 1466–1478.
Kuo, L.-J., Louchouarn, P., Herbert, B.E., 2011a. Influence of combustion conditions on yields of solvent-extractable anhydrosugars and lignin phenols in chars: Implications for characterizations of biomass combustion residues. Chemosphere 85, 797–805.
Kuo, L.-J., Louchouarn, P., Herbert, B.E., Brandenberger, J.M., Wade, T.L., Crecelius, E., 2011b. Combustion-derived substances in deep basins of Puget Sound: historical inputs from fossil fuel and biomass combustion. Environmental Pollution 159, 983–990.
Lai, C., Liu, Y., Ma, J., Ma, Q., He, H., 2014. Degradation kinetics of levoglucosan initiated by hydroxyl radical under different environmental conditions. Atmospheric Environment 91, 32–39.
Longmore, M.E., 1997. Quaternary palynological records from perched lake sediments, Fraser Island, Queensland, Australia: rainforest, forest history and climatic control. Australian Journal of Botany 45, 507–526.
Longmore, M.E., Heijnis, H., 1999. Aridity in Australia: Pleistocene records of palaeohydrological and palaeoecological change from the perched lake sediments of Fraser Island, Queensland, Australia. Quaternary International 57, 35–47.
Lopes dos Santos, R.A., De Deckker, P., Hopmans, E.C., Magee, J.W., Mets, A., Damsté, J.S.S., Schouten, S., 2013. Abrupt vegetation change after the Late Quaternary megafaunal extinction in southeastern Australia. Nature Geoscience 6, 627–631.
Marlon, J.R., Kelly, R., Daniau, A.-L., Vannière, B., Power, M.J., Bartlein, P., Higuera, P., Blarquez, O., Brewer, S., Brücher, T., 2016. Reconstructions of biomass burning from sediment charcoal records to improve data-model comparisons. Biogeosciences 13, 3225–3244.
Matthias, I., Giesecke, T., 2014. Insights into pollen source area, transport and deposition from modern pollen accumulation rates in lake sediments. Quaternary Science Reviews 87, 12–23.
McNiven, I.J., Thomas, I., Zoppi, U., 2002. Fraser Island Archaeological Project (FIAP): background, aims and preliminary results of excavations at Waddy Point 1 Rockshelter. Queensland Archaeological Research 13, 1–20.
Mooney, S., Tinner, W., 2011. The analysis of charcoal in peat and organic sediments. Mires and Peat 7, 1–18.
Moss, P.T., Tibby, J., Petherick, L., McGowan, H., Barr, C., 2013. Late Quaternary vegetation history of North Stradbroke Island, Queensland, eastern Australia. Quaternary Science Reviews 74, 257–272.
Myers-Pigg, A.N., Griffin, R.J., Louchouarn, P., Norwood, M.J., Sterne, A., Cevik, B.K., 2016. Signatures of biomass burning aerosols in the plume of a saltmarsh wildfire in South Texas. Environmental Science & Technology 50, 9308–9314.
Myers-Pigg, A.N., Louchouarn, P., Teisserenc, R., 2017. Flux of dissolved and particulate low-temperature pyrogenic carbon from two high-latitude rivers across the spring freshet hydrograph. Frontiers in Marine Science 4, 38.
Pratap, V., Chen, Y., Yao, G., Nakao, S., 2018. Temperature effects on multiphase reactions of organic molecular markers: A modeling study. Atmospheric Environment 179, 40–48.
Prentice, I.C., 1985. Pollen representation, source area, and basin size: toward a unified theory of pollen analysis. Quaternary Research 23, 76–86.
Rieley, G., Collier, R.J., Jones, D.M., Eglinton, G., Eakin, P.A., Fallick, A.E., 1991. Sources of sedimentary lipids deduced from stable carbon-isotope analyses of individual compounds. Nature 352, 425–427.
Schefuß, E., Ratmeyer, V., Stuut, J.-B.W., Jansen, J.F., Sinninghe Damsté, J.S., 2003. Carbon isotope analyses of *n*-alkanes in dust from the lower atmosphere over the central eastern Atlantic. Geochimica et Cosmochimica Acta 67, 1757–1767.
Schreuder, L.T., Hopmans, E.C., Stuut, J.-B.W., Damsté, J.S.S., Schouten, S., 2018. Transport and deposition of the fire biomarker levoglucosan across the tropical North Atlantic Ocean. Geochimica et Cosmochimica Acta 227, 171–185.
Schüpbach, S., Kirchgeorg, T., Colombaroli, D., Beffa, G., Radaelli, M., Kehrwald, N.M., Barbante, C., 2015. Combining charcoal sediment and molecular markers to infer a Holocene fire history in the Maya Lowlands of Petén, Guatemala. Quaternary Science Reviews 115, 123–131.
Schwark, L., Zink, K., Lechterbeck, J., 2002. Reconstruction of postglacial to early Holocene vegetation history in terrestrial Central Europe via cuticular lipid biomarkers and pollen records from lake sediments. Geology 30, 463–466.
Shafizadeh, F., Furneaux, R.H., Cochran, T.G., Scholl, J.P., Sakai, Y., 1979. Production of levoglucosan and glucose from pyrolysis of cellulosic materials. Journal of Applied Polymer Science 23, 3525–3539.
Shanahan, T.M., Hughen, K.A., McKay, N.P., Overpeck, J.T., Scholz, C.A., Gosling, W.D., Miller, C.S., Peck, J.A., King, J.W., Heil, C.W., 2016. CO_2 and fire influence tropical ecosystem stability in response to climate change. Scientific Reports 6, 29587.
Shiraiwa, M., Pöschl, U., Knopf, D.A., 2012. Multiphase chemical kinetics of NO_3 radicals reacting with organic aerosol components from biomass burning. Environmental Science & Technology 46, 6630–6636.
Sikes, E.L., Medeiros, P.M., Augustinus, P., Wilmshurst, J.M., Freeman, K.R., 2013. Seasonal variations in aridity and temperature characterize changing climate during the last deglaciation in New Zealand. Quaternary Science Reviews 74, 245–256.
Simoneit, B.R., Elias, V.O., 2000. Organic tracers from biomass burning in atmospheric particulate matter over the ocean. Marine Chemistry 69, 301–312.
Simoneit, B.R., Schauer, J.J., Nolte, C., Oros, D.R., Elias, V.O., Fraser, M., Rogge, W., Cass, G.R., 1999. Levoglucosan, a tracer for cellulose in biomass burning and atmospheric particles. Atmospheric Environment 33, 173–182.
Sugita, S., 1994. Pollen representation of vegetation in Quaternary sediments: theory and method in patchy vegetation. Journal of Ecology, 881–897.
Ulm, S., 2011. Coastal foragers on southern shores: Marine resource use in northeast Australia since the late Pleistocene. In: Bicho, Nuno F., Haws, Jonathan A., Davis, Loren G. (Eds.), Trekking the Shore. Springer, pp. 441–461.
Vachula, R.S., Russell, J.M., Huang, Y., Richter, N., 2018. Assessing the spatial fidelity of sedimentary charcoal size fractions as fire history proxies with a high-resolution sediment record and historical data. Palaeogeography, Palaeoclimatology, Palaeoecology 508, 166–175.
Walker, J., Thompson, C., Fergus, I., Tunstall, B., 1981. Plant succession and soil development in coastal sand dunes of subtropical eastern Australia. In: West, Darrel C., Shugart, Herman H., Botkin, Daniel B. (Eds.), Forest Succession. Springer, New York, pp. 107–131.
Webb, L., Tracey, J., 1994. The rainforests of northern Australia. In: Groves, R.H. (Ed.), Australian Vegetation. Cambridge University Press, Cambridge, pp. 87–129.
Whitlock, C., Larsen, C., 2002. Charcoal as a fire proxy. In: Smol, John P., John, H., Birks, B., Last, William M., Bradly, Raymond S., Alverson, Keith (Eds.), Tracking Environmental Change Using Lake Sediments. Springer, Dordrecht, pp. 75–97.
Zhao, R., Mungall, E.L., Lee, A.K., Aljawhary, D., Abbatt, J.P., 2014. Aqueous-phase photooxidation of levoglucosan–a mechanistic study using aerosol time-of-flight chemical ionization mass spectrometry (Aerosol ToF-CIMS). Atmospheric Chemistry and Physics 14, 9695–9706.